Journal of Sustainability Science and Management
Volume 17 Number 3, March 2022: 145-160
eISSN: 2672-7226

ANALYSIS OF SEDIMENT RATING CURVE AND SEDIMENT LOAD FOR LANGAT RIVER BASIN

WEI-KOON LEE[1*], TUAN ASMAA TUAN RESDI[1] AND JUWITA ASFAR[2]

[1]School of Civil Engineering, College of Engineering, Universiti Teknologi MARA (UiTM), 40450 Shah Alam, Selangor, Malaysia. [2]School of Civil Engineering, College of Engineering, Universiti Teknologi MARA (UiTM), Cawangan Johor, Kampus Pasir Gudang, 81750 Masai, Johor, Malaysia.

**Corresponding author: leewei994@uitm.edu.my*
Submitted final draft: 3 July 2020 *Accepted: 28 September 2020* http://doi.org/10.46754/jssm.2022.03.012

Abstract: An analysis of suspended sediment and streamflow over a period of 12 months in three monitoring stations, FS1, FS2 and FS4, from the upstream to downstream of the Langat River was carried out. The statistical approach and examination of the physical process aim to provide a better understanding of the sediment flow characteristics. The objective is to evaluate the sediment rating curves to estimate the suspended sediment concentration (SSC), hence the seasonal and annual sediment load. Correlations improve when the streamflow lead sediment is discharged by one day. In addition, the concave sediment rating curve indicates resuspension of deposited materials in the river system during flood. A plot of SSC and flow duration curve shows the increase of sediment sources at the basin in the downriver direction and outliers are attributed to flash floods. Log-transformed linear regression of sediment concentration rating curve gives the best R^2 values and the lowest percent mean error for all stations. The total annual sediment load in the river basin upstream of FS4 is estimated to be 657,551 tonnes, where the monthly and seasonal variations are consistent with the monsoon period. Stations FS2 and FS4 have approximately the same sediment yield, but the concentration reduces downstream due to flow dilution effect. The model works well for the prediction of sediment discharge of regular flows but may overestimate annual sediment yield due to high flows. The present study contributes to more precise prediction of sediment loading in a river basin for related engineering application.

Keywords: Langat River basin, sediment rating curves, sediment yield, suspended sediment, regression analysis.

Introduction

Soil erosion is a natural process that continuously occurs without any symptom or warning signs. However, due to uncontrolled development, it has increasingly become a serious issue and is predicted to become an even more critical issue in the future (Zainal Abidin *et al.,* 2017). Soil erosion causes not only soil nutrient loss and land degradation, but also leads to many secondary problems attributed to the sediment and sedimentation process, such as river siltation, water pollution, and flooding (He & Jiao, 1998; Munodawafa, 2007; Rahman *et al.,* 2009; Rickson, 2013). Excessive soil erosion is a serious threat to sustainable development of resources and the environment. Therefore, monitoring and evaluation of soil erosion is particularly important.

The erosion process begins with the impact energy due to rainfall, causing exposed soil mass to be dislodged. Subsequently, the eroded mass is transported in the form of sediment by surface runoff into the river system (Atkinson, 1995). The sediment load in the river is carried by the stream flow power. The sediment may be carried downstream as bed load, which moves along the riverbed by rolling, skipping, or sliding, or in the form of suspended load, fully supported by fluid flow and maintained by fluid turbulence (Yang, 2003). Bed load is flow-dependent, difficult to measure, but relatively easy to predict (Wang & Ren, 1998). A river's suspended load depends on source environments and supply conditions and may be deposited when the stream power is too low. The natural correlation between the flow discharge and the sediment flow rate becomes

more pronounced during extreme events related to intense rainfall and high river flows (Tfwala & Yu, 2016).

However, sediment transport cannot be viewed as a simple function of hydraulic conditions because many other factors influence this relationship, including boundary shear, temperature, bed roughness and the fall velocity of the bed material.

In general, erosion and sedimentation rates are highly variable in response to climate and human influences (Nyssen *et al.,* 2003). Vegetative cover, drainage basin geology, level of glaciation, rainfall intensity, climate trends, topographic relief, and man's impact are all known to influence the rate of sediment production and transport (Wang & Ren, 1998; Millman & Meade, 1983). Although they cannot be measured directly, they can be estimated or analysed based on the variations of suspended sediment flow rate in the river. Understanding river flows and the transport pathways of sediment is thus crucial to the analysis of erosional and depositional landscapes (Allen, 2008).

Generally, there are three main categories of sediment yield or load calculation models, which are empirical or statistical, conceptual, and physical-based models. Merritt *et al.* (2003) summarised these models in terms of their classification, input data requirements and scales of application, and concluded that model components generally contain a mix of empirical, physic-based algorithms, and conceptual models. The prediction of suspended sediment yield in medium and large catchments requires high quality hydrological and environmental data, which typically may be unavailable (Letcher *et al.,* 1999).

According to Mount and Abrahart (2011), the sediment rating curve approach, *sensu stricto*, is applicable only to the analysis of measured values of discharge and concentration, which are frequently treated as daily averages. Such a relationship is usually established by regression analysis of the time series observations obtained from a permanent river monitoring station. Sediment rating curves are generally expressed in the form of a power-law type equation, log transformed linear equation or polynomial function (Hassan, 2014; De Girolamo *et al.,* 2015). When continuous sampling at short intervals is performed, a time series analysis or artificial neural networks with consideration of autocorrelation may produce the best result (Moatar & Meybeck, 2005).

The Langat River basin is one of the important river basin in the state of Selangor, which is experiencing a significant spillover development effect from the Klang Valley. Previous studies related to its sediment rating curve have been conducted, where artificial neural network was employed to investigate the non-linear behaviour of the suspended sediment flow (Ab. Ghani, 2011; Memariana *et al.,* 2013). Despite the powerful trend recognition algorithm of artificial neural network and its readiness for prediction application, a thorough investigation of the statistics and underlying physical process is crucial to better understand the sediment flow in this basin. The objectives of this study are to evaluate the sediment rating curves for the purpose of estimating suspended sediment concentrations in the river and subsequently estimate the annual and seasonal sediment load from the upstream of the contributing catchment.

Materials and Methods

Study Area

The Langat River basin is situated at the boundary of the states of Selangor and Negeri Sembilan, within the latitude 2° 40'N to 3° 20'N and longitude 101° 10'E to 102° 00'E, with a total catchment area of approximately 2,394 km^2. The major tributaries in the basin are Semenyih River and Labu River, which converges to Langat River (Figure 1). The basin land use is primarily agricultural (55.13%), followed by forest (19.31%), wetland and swamps (12.73%), urban built-up areas (6.20%), mining (1.61%) and other activities (5.02%).

For the area within 1 km from the main river, nearly half (47%) of the land use is dominated by cash crops (e.g. rubber plantation and palm oil), 17% is municipal and residential use, and 10% is mixed plantation (e.g. orchards, banana, coconuts etc) (Zainal Abidin *et al.,* 2018).

The Langat River basin can be subdivided into three distinct zones, namely, the mountainous zone located at the northeast region of Hulu Langat, the hilly area located in the middle part of the basin and the flat alluvial plane located at the southwest near the river mouth, which connects to the Straits of Malacca. The river sediment composition changes gradually from boulder/gravel in the mountainous zone, to sand and silt in the hilly areas, whereas most of the flat alluvial plane area is characterised by peat with clay and silt soil.

For the purpose of this study, three stations located along the western branch of the middle Langat River are considered, namely, from the upstream to downstream, Stations FS1 Sg Lui (03° 10' 25" N 101° 52' 20" E), FS2 Sg Langat in Kajang (02° 59' 40" N 101° 47' 10" E), and FS4 Sg Langat in Dengkil (02° 59' 34" N 101° 47' 13" E). Station FS3 on a separate tributary is not considered. The stations are operated and maintained by the Department of Irrigation and

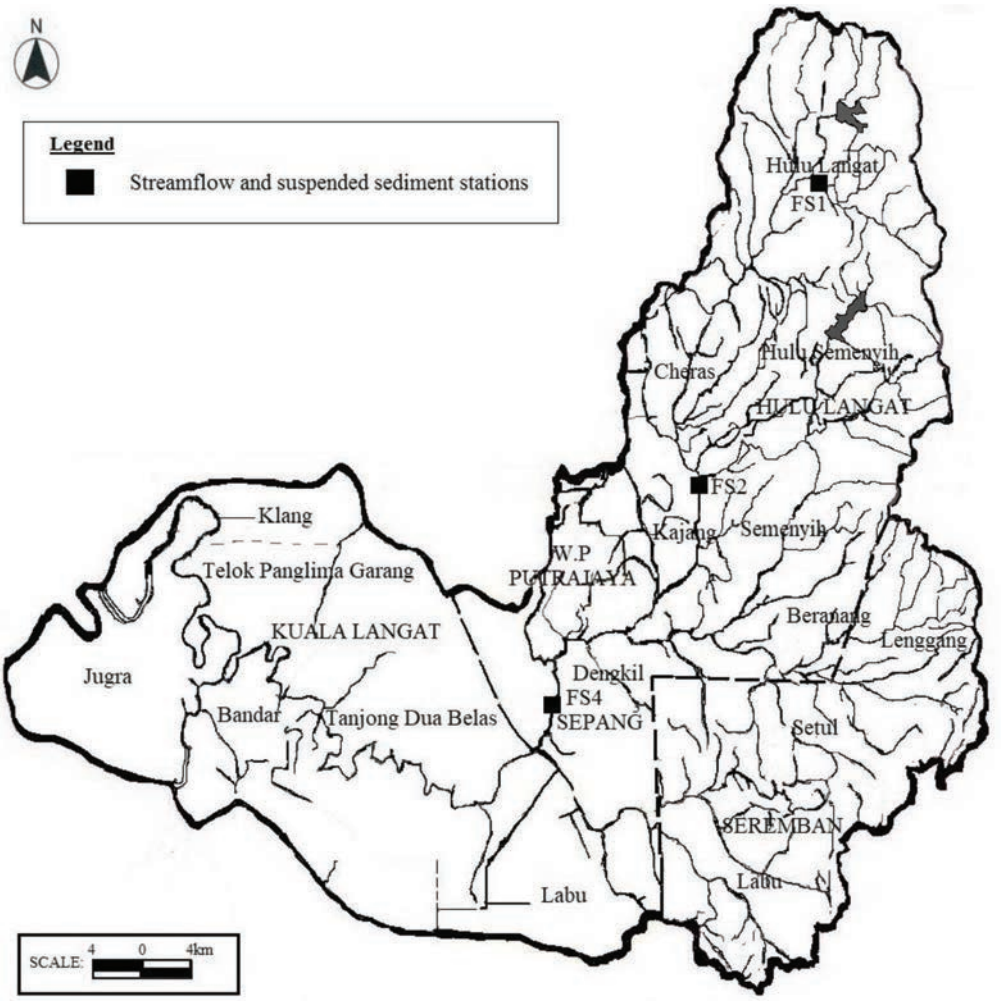

Figure 1: Location of the streamflow and suspended sediment stations in the Langat River basin

Drainage Malaysia (DID), Malaysia, of which the streamflow and suspended sediment data were collected on daily basis using float devices and bottle sampling, respectively. The secondary sediment data from DID is only available for the period from 2006 to 2008. For the purpose of this study, the daily data for the year 2006 is analysed and data for years 2007 and 2008 were used for validation.

Methodology

In the present study, the raw data is the streamflow SF (or Q_s in m^3/s) and the sediment discharge SD (or Q_s/Q in ton/day).

The suspended solid concentration SSC (or in general C) can be derived from (in ton/m^3) and empirically correlated to the independent variable streamflow using a power function (De Girolamo *et al.,* 2015):

$$C = aQ^b + \varepsilon \quad (1a)$$

where a, b are constants, and the error term is normally distributed and additive on the arithmetic scale. Equation (1a) can be cast in the form of log-transformed to be modelled using linear regression, where the error term is normally distributed and additive on the logarithmic scale (Xio *et al.,* 2011), giving:

$$\log C = \log a + b \log Q + \varepsilon \quad (1b)$$

The different assumptions about how stochasticity manifests in the model means the error term in Equation (1b) is log-normally distributed, multiplicative error on the arithmetic scale:

$$C = aQ^b e^{\varepsilon} \quad (1c)$$

Mathematically, only one of the above assumptions can be correct for a single data set. Xio *et al*. (2011) stated that where the error is approximately multiplicative log-normal, the log-transformed linear regression should be used, while non-linear regression on untransformed data should be applied to data sets with additive normal error.

Another alternative regression equation is the second-order polynomial expansion of the log-transformed variates in the form below:

$$\log C = \log a + b \log Q + c(\log Q)^2 + \varepsilon \quad (1d)$$

Applicability of the above equations depend very much on the error structure of the data set. Hence, to produce high-quality regression, the high, intermediate and low flow regions may be separately treated to improve the *C-Q* correlation.

Following Phillips *et al.* (1999), a smearing correction factor *CF* is applied to the back-log transformed data using the following equation:

$$CF = \frac{1}{N}\sum_1^N 10^{\varepsilon_i} \quad (2)$$

where

$$\varepsilon_i = \log(C_i) - \log(C_i') \quad (3)$$

is the residual between the log-transformed measured concentration and predicted values and N is the number of observation. The percent mean error E is evaluated as follows (Horowitz, 2003):

$$E(\%) = \frac{1}{N}\sum_1^N \left(\frac{C_i' - C_i}{C_i}\right) \times 100 \quad (4)$$

The *C-Q* relationships (rating curves) can be used to evaluate the average load L passing through a river cross-section during a time interval ($\Delta t = t_2 - t_1$), given mathematically as:

$$L = \int_{t_1}^{t_2} Q_t C_t \mathrm{d}t \quad (5)$$

where Q_t is the streamflow at time t, and is the suspended solid concentration. The results can be further aggregated on different time scales: month, season and year.

Results and Discussion

Missing Data

Figure 2 shows the combined plot of the streamflow (SF) and suspended sediment discharge (SD) in year 2006 for stations FS1, FS2 and FS4, respectively. There is substantial missing data in the second half of the year for FS2 due to instrument issues. However, for the purpose of this study, the missing data is ignored and only available data were analysed.

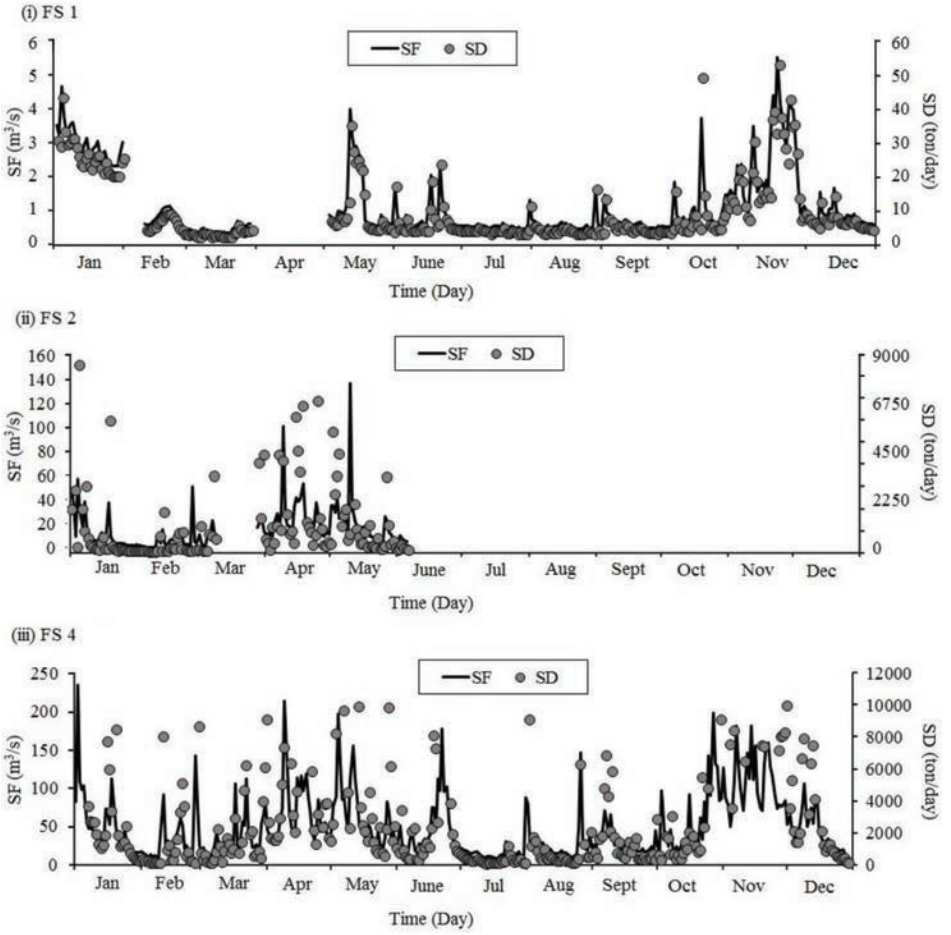

Figure 2: Suspended sediment and stream flow for year 2006

SD-SF Power Law Regression

In Figure 3a, the power law regression between the SF and SD are first examined. For all three stations, the results show very poor correlations, except for FS1 ($R^2 = 0.828$), which approximated a linear behaviour. FS1 is located on the upstream of the river basin in a tributary near Langat Dam, but not immediately on the downstream of the dam release path. Thus, it provides a good indication of sediment yield from the upper Langat River basin. The good correlation for FS1 is likely representative of the natural correlation relatively free from human intervention.

However, the trend deteriorates with the downstream stations FS2 and FS4, suggesting that basin land use and cover management practices may have caused an increase or reduction in sediment flow in the fluvial system. Furthermore, localised sink attributed to deposition in the downriver reaches may have also contributed to the disparity. For FS4, there are observations of null SD values during some of the flood events, which may be attributed to instrument error.

Outliers Detection

Inspection of the data sets shows outliers that are quite different from rest of the observations, which may have significantly affected the data processing (Mishra & Soni, 2019). We define outliers as data points with standard regression

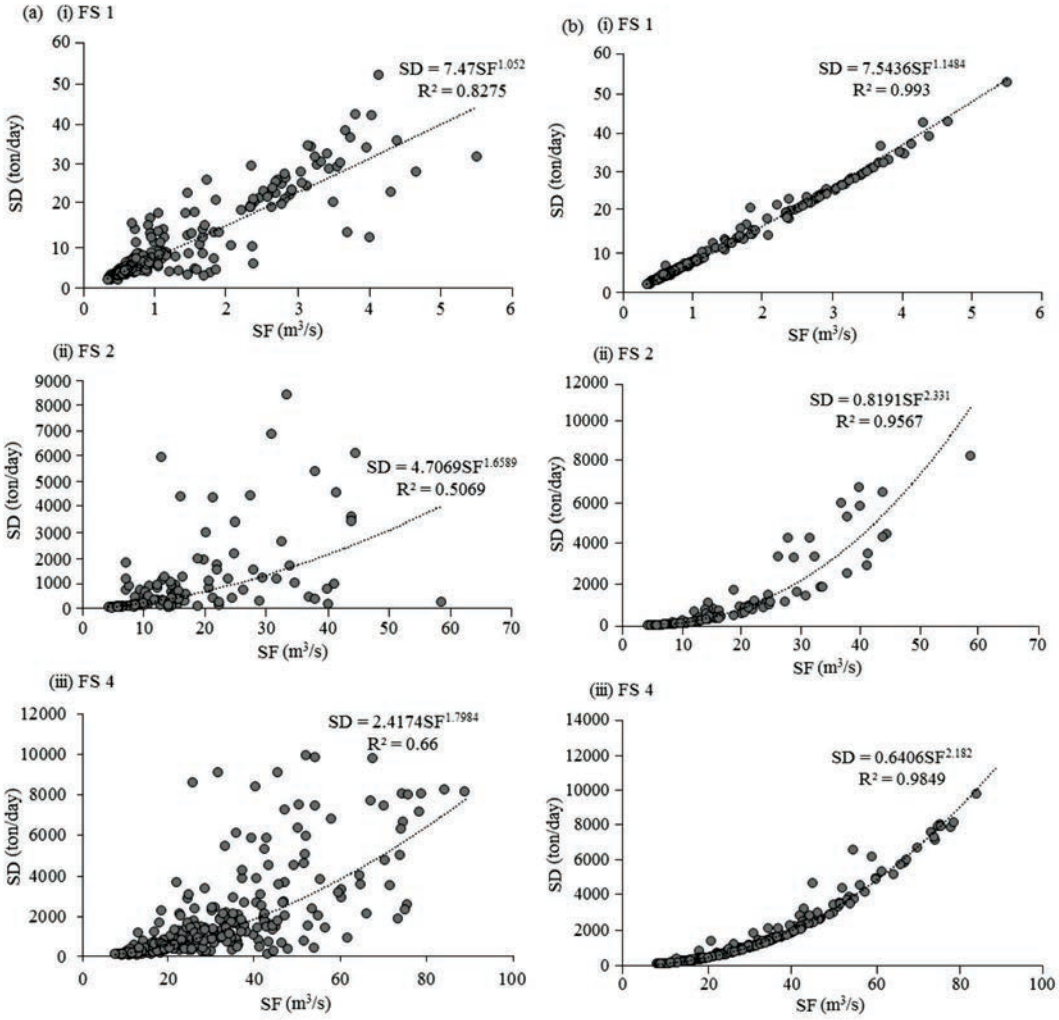

Figure 3: Power law regression of suspended sediment discharge and streamflow: (a) no time-shift, (b) SF lead SD by 1 day

residual larger than ±2. Analysis shows that the percentages of outliers for all three stations are in the order of 7%, totalling 22 nos. and 21 nos. for FS1 and FS3, respectively and 10 nos for FS2. However, we did not remove the outliers at this stage and proceeded to examine the time-shift patterns in the data sets as discussed in the next section.

SD-SF Time Shift

The lead or lag behaviour of maximum sediment flow with respect to flood wave is a common observation, but are not always taken into consideration by researchers (Balamurugan, 1989). Based on this premise, we repeated the power law regression of the two data sets by offsetting SD with respect to SF. The results as shown in Figure 3b show that the correlation improves significantly if SF leads by 1 day, with the R^2 values being 0.993 (FS1), 0.957 (FS2) and 0.985 (FS4). This suggests that the observation of peak flow discharge precedes the peak sediment discharge. Note that if hourly data sets are available, a more accurate lead time can then be determined accordingly (Heng

& Suetsugi, 2015). The concave shape of the sediment rating curve may also suggest prompt resuspension of previously deposited materials in the river system as flood discharge increases (Heng & Suetsugi, 2015).

At this stage, we repeated the outlier test and identified the number of outliers to have reduced considerably when SF lead SD by 1 day. The total numbers of data points removed for FS1, FS2 and FS4 are 14 (3.8%), 1 (0.8%) and 14 (4.7%) respectively.

Hysteresis of Sediment Rating Curve

The delayed observation of sediment peak compared with flow peak suggests the longer concentration time required for sediment movement. The lag of peak sediment discharge is typically associated with the travelling time between the sediment supply (the basin interior) and the monitoring site (river sampling station). This suggests sediment sources are spread out within the catchment, where the dynamics are much slower than the streamflow, producing an anti-clockwise hysteresis effect (Figure 4),

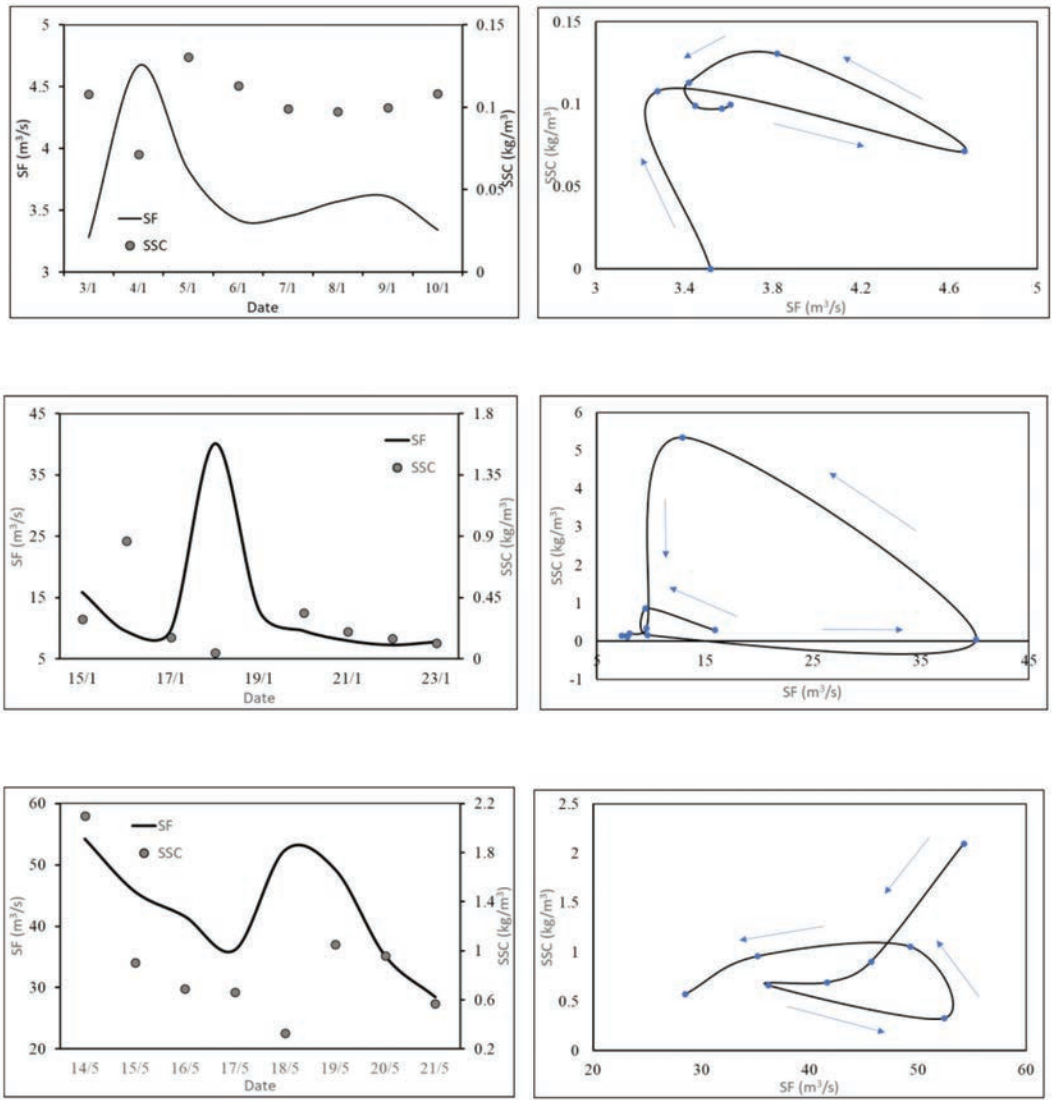

Figure 4: Hysteresis plots for flood events (FS1, FS2 and FS4)

consistent with observation by De Girolamo *et al.* (2015). Yang and Lee (2018) attributed the smaller sediment concentration on the rising limb of the hydrograph to the relative travel time of the flood wave and the sediment flux, high soil erodibility during flooding and seasonal variability of rainfall, and the sediment production.

Data Statistical Distribution

Next, the statistical distribution of the SF and SD data series is examined. Table 1 shows that the logarithmic series has excess kurtosis closer to 0 and negligible skewness, suggesting that linear regression on the log-transformed series (Equation 1b) should yield better correlation compared with the power law (Equation 1a).

To further validate the above, we tested normality using the Shapiro-Wilk test. The W-value for SF and SD for the respective stations are 0.032 and 0.027 for FS1, 0.034 and $1.2x10^{-5}$ for FS2, and 0.317 and 0.002 for FS4. In all cases, the p-value approaches zero, hence suggesting that the data sets are not normally distributed.

SSC Log-transformed Linear Regression

Figure 5(a) and (b) shows linear regression of the log-transformed suspended sediment load and concentration curve, respectively. The R^2 values of the sediment load rating curve is well above 0.95, but below 0.95 and not less than 0.7 for the concentration rating curve. This shows that the daily sediment load is strongly correlated to the 1-day lead streamflow, but sediment concentration may vary due to large disparity between regular and flood events.

SSC Distribution with Flow Duration Curve (FDC)

The distribution of the suspended sediment concentration SSC under varying flow magnitude can be examined by plotting SSC in correspondence with the flow duration curve (FDC) (Figure 6). Following De Girolamo *et al.* (2015), the FDCs are subdivided into the high flow region for <20% exceedance and the low flow region for >70% exceedance. In the case of the three stations considered, the FDCs only show mild changes in curvature in the high and low flow regions relative to the intermediate region. For FS1, it is observed that there is only nominal increase in sediment concentration during a high flow event. For FS2, a number of outliers that represent the values during flash flood events can be observed.

For FS4, the sediment concentration sees an increase at a much higher rate compared with the other two stations as SSC rises from 0.01 to 0.75 kg/m^3 when flow magnitude increases from 100% exceedance to <10% exceedance. An even much steeper rise in SSC occurs in the last 10 percentile of the streamflow and a number of outliers can also be observed throughout the record.

Table 1: Kurtosis (excess) and skewness of data series

	FS1		FS2		FS4	
	SF	**SD**	**SF**	**SD**	**SF**	**SD**
Original Series						
Kurtosis	2.701	3.369	1.451	5.981	.949	4.835
Skewness	1.842	1.944	1.331	2.479	1.130	2.221
Log-transformed series						
Kurtosis	-.178	-.274	-.798	-.899	-.652	-.671
Skewness	.984	.887	.177	.210	.048	.059

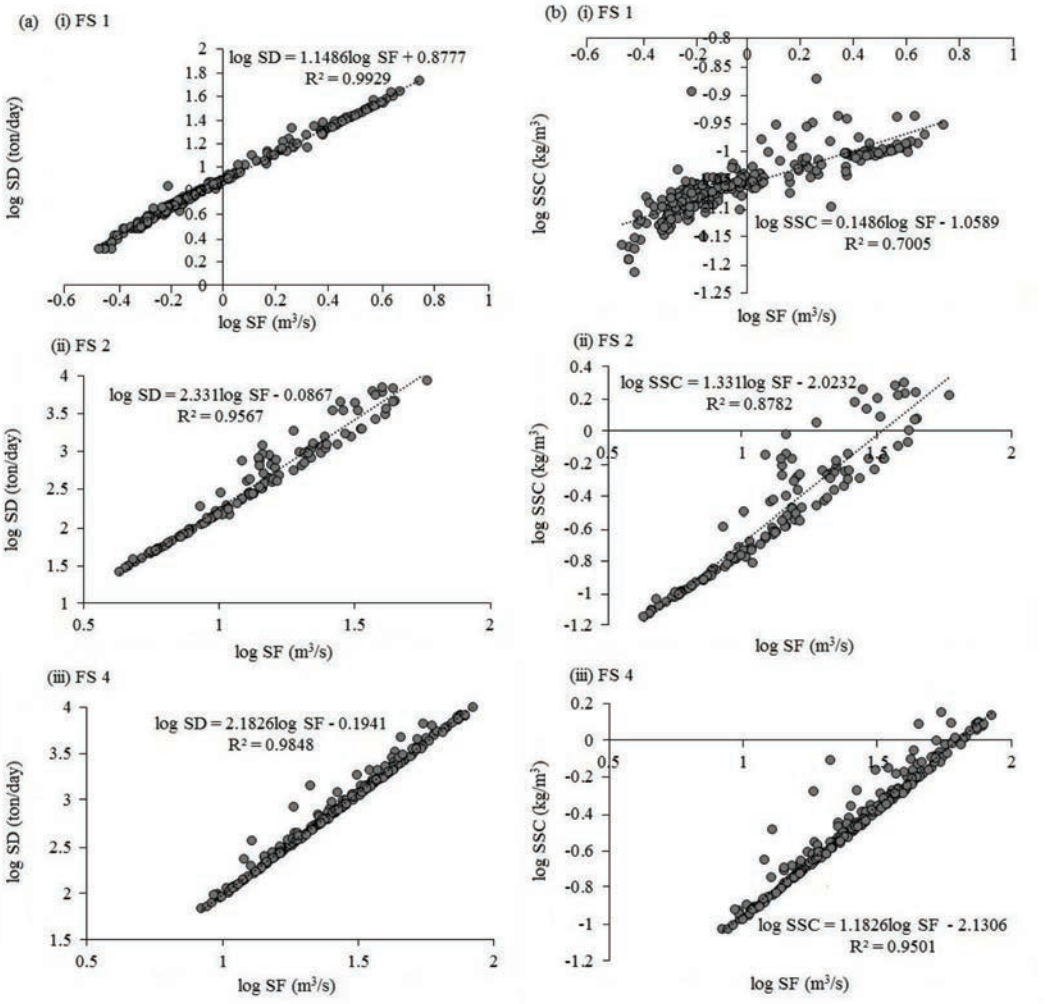

Figure 5: Linear regression curve for the log-transformed data: (a) sediment load, and (b) sediment concentration rating curve

Sediment Concentration Range

Table 2 shows the maximum, minimum and range of sediment concentration observed in the three stations. The minimum sediment concentration increases marginally (14.8%) from FS1 to FS2, and by up to 32.9% from FS2 to FS4 due to the accumulation of sediment materials in the downriver direction during regular events. The maximum sediment concentration observed in FS1 is more than double the minimum value, but still relatively low at 0.134 kg/m^3, suggesting minimum sediment sources in its catchment. Meanwhile, maximum sediment concentrations in FS2 and FS4 during flood events increas significantly (over 2700% and 1400%, respectively) compared with regular events. This shows that the catchment area of FS2 has abundant sediment sources. However, the lower maximum sediment concentration at FS4 compared with FS2 may suggest dilution effect due to higher downstream streamflow.

Best Regression Model

Table 3 summarises the log-transformed linear regression result, correction factors and percent mean error for the three stations. The R^2 value is

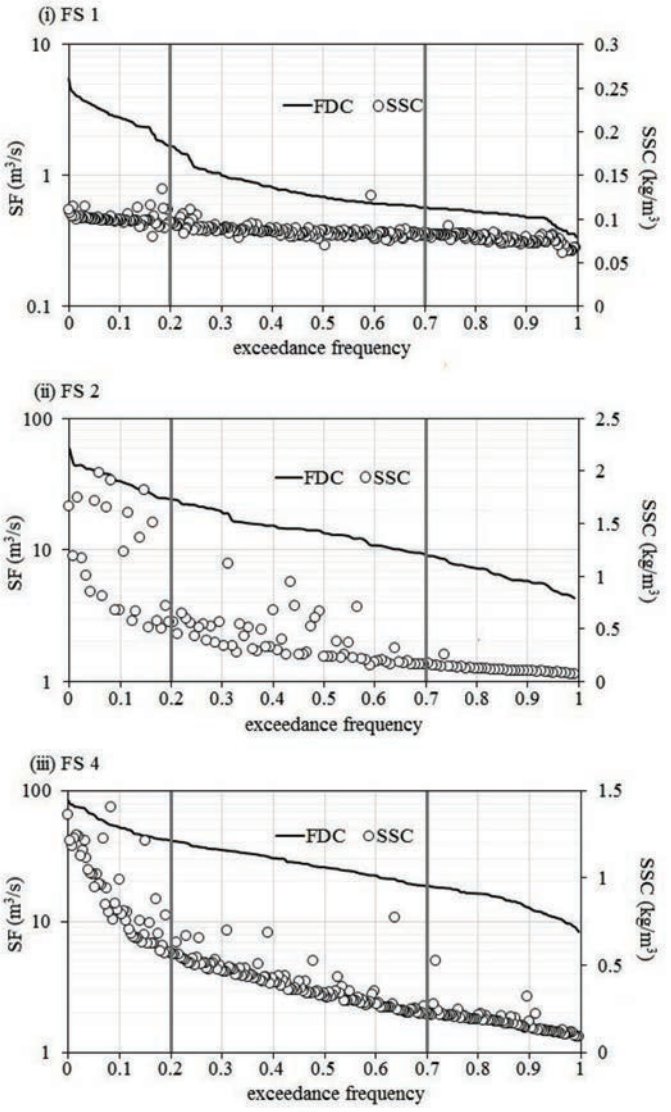

Figure 6: The suspended sediment concentration distributions with the flow duration curves

Table 2: Variation of sediment concentration

C (kg/m³)	FS1	FS2	FS4
Maximum Value	0.134	1.986	1.403
Minimum Value	0.061	0.070	0.093
Range	0.073	1.916	1.310

the highest for FS4 at above 0.925, whereas the values FS1 and FS2 are above 0.70. Except for FS1, the R^2 values of the linear and polynomial log-transformed equations show negligible difference. For FS1, the log-transformed polynomial equation yields the best correlation and lowest error. For FS2 and FS4, the log-transformed linear equation yields the lowest

Table 3: Regression coefficients, percentage error and correction factor of sediment concentration rating curves

Equation		FS1	FS2	FS4
Power Curve	a	0.087	0.010	0.007
$SSC = aSF^b$	b	0.148	1.331	1.182
	R^2	0.703	0.712	0.925
	E(%)	-.156	10.104	-4.794
Log-transformed	a	0.149	1.331	1.183
(linear)	b	-1.059	-2.023	-2.131
$\log SSC = a \log SF + b$	R^2	0.701	0.878	0.950
	CF	1.006	1.156	1.069
	E(%)	-.162	-.906	-4.483
Log-transformed	a	-.143	-.083	0.031
(polynomial)	b	0.174	1.524	1.094
$\log SSC = a (\log SF) + b \log SF + c$	c	-1.046	-2.128	-2.069
	R^2	0.746	0.879	0.950
	CF	1.002	1.164	0.960
	E(%)	0.127	-1.642	6.404

error. The correction factor *CF* to account for smearing due to back-log transformation is the lowest for FS1, followed by FS4, and up to the order of 1.16 for FS2. From the evaluation above, it is concluded that the linear log-transformed equation gives the best data correlation and is thus suitable for predictive purpose, and especially so for FS4, which is of more interest due to its location further downstream in the basin.

Temporal Sediment Load Variation

The monthly sediment load variation in FS4 is examined (Figure 7). FS4 is the most downstream station and is also most susceptible to summative effect of basin changes in the upstream. The total monthly load increases in April and November in conjunction with the monsoon. The minimum and average monthly values generally follow the same trend. A corresponding maximum sediment load is

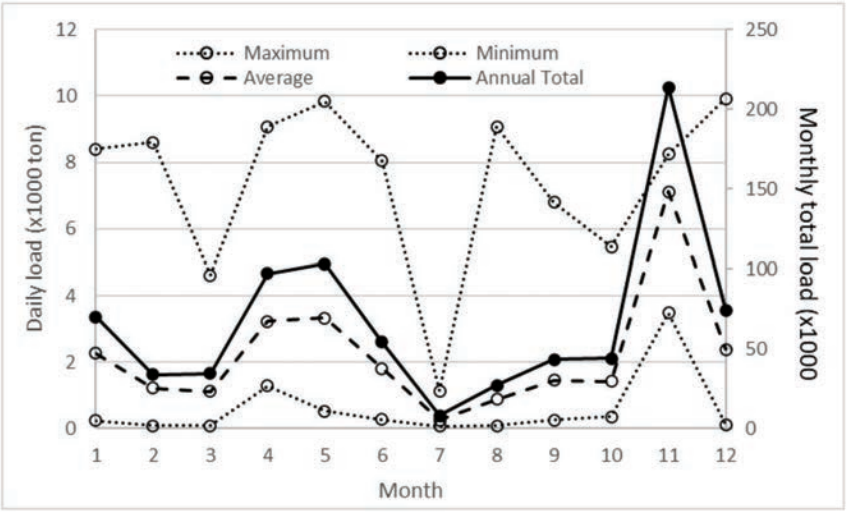

Figure 7: Monthly sediment load variation in FS4 (2006)

observed in May and December. Overall, the maximum sediment load remains relatively high, possibly due to flash flood events, and only falls below 5,000 tonnes/day in March and July. The average daily sediment load ranges between 300 tonnes/day to 3,300 tonnes/day throughout the year, but spikes above 7,000 tonnes/day in November.

Table 4 shows the daily maximum, minimum, average and total sediment load in the three stations calculated for every 3-month period and for the entire year of 2006. For FS2, the data covers only the first and second quarters of the year. The seasonal sediment load for the second half of the year is estimated, but daily maximum and minimum is omitted due to the actual past streamflow record being unavailable.

The sediment load at FS1 is, in general, well below 1% of FS4; the sediment load at FS2, meanwhile, lies between 40% and 50% of FS4, based on which estimates for the third and fourth quarters and the entire year are made. The approximate doubling of total sediment load from FS2 to FS4 also suggests the total sediment loads from their respective catchment are identical. This observation is consistent with the change in sediment concentration in Table 2. In summary, the total sediment load from the Langat River basin area upstream of FS4 in 2006 amounts to 657,551 tonnes per year.

Sediment Load Prediction

Using the correlation derived in Table 3, the sediment discharge and sediment load for FS4 from 2006 to 2008 are determined. Figure 8 shows the predicted and the observed SD for 2008, which are in excellent agreement, except during high flow events in April and October.

Table 5 summarises the R^2 values for SD prediction, where it is above 0.9 for 2006, but drops to 0.79 and 0.69 for 2007 and 2008, respectively. However, the R^2 values improve significantly, and even rise above 0.9, for 2008 if only regular events below 2000 tonnes/day

Table 4: Sediment load (tonne) in the Langat River basin

		Sediment Load (tonne)		
		FS1	**FS2**	**FS4**
January-March	Daily Max.	43.1	8456.3	8598.1
	Daily Min.	2.0	26.0	88.3
	Daily Ave.	12.5	700.7	1513.5
	Total	**1,111**	**54,693**	**134,370**
April-June	Daily Max.	35.0	6863.0	9833.9
	Daily Min.	3.7	107.4	274.0
	Daily Ave.	8.6	1420.4	2723.2
	Total	**783**	**119,196**	**247,809**
July-September	Daily Max.	16.1	-	9073.7
	Daily Min.	3.0	-	67.7
	Daily Ave.	4.3	416.2*	867.0
	Total	**394**	**37,981***	**79,761**
October-December	Daily Max.	52.9	-	9909.5
	Daily Min.	3.4	-	123.3
	Daily Ave.	12.2	1113.4*	2708.0
	Total	**1,134**	**101,596***	**253,991**
Annual	Daily Max.	52.9	8456.3*	9909.5
	Daily Min.	2.0	26.0*	67.7
	Daily Ave.	9.3	858.8*	1802.0
	Total	**3,390**	**313,467***	**657,551**

*proportioned based on FS4

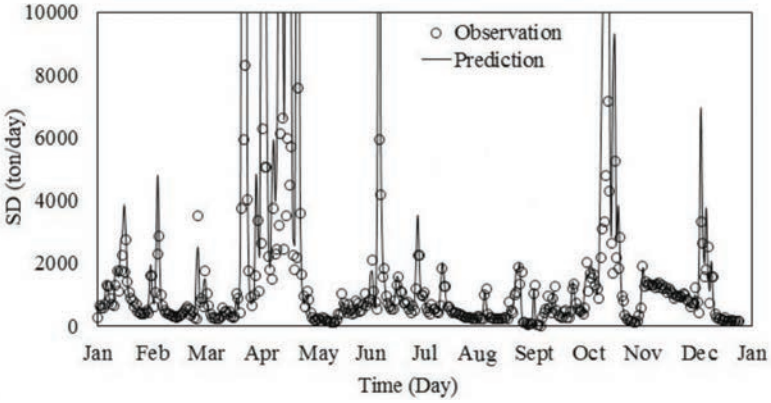

Figure 8: Predicted and observed sediment discharge at FS4 for year 2008

Table 5: Sediment load prediction for FS4 (year 2006-2008)

	2006	**2007**	**2008**
R^2 (overall)	0.91	0.79	0.69
R^2 (SD<2000 ton/d)	-	0.85	0.91
MSE (SD<2000 ton/d)	0.024	0.048	0.004
Annual load (ton)	657,551	1,219,833	901,763
Average SF (m^3/s)	48.9	42.4	33.6
Maximum SF (m^3/s)	234	186	243

are considered. This shows that the errors in the predictive model are primarily attributed to extreme events. The estimated annual sediment load is not strongly correlated to the average and maximum streamflow, indicating the error associated with high flow events are likely to affect catchment sediment yield estimation.

We further compared the predictions of the log-transformed linear equation to the power law and log-transformed polynomial equations, and the calculated Nash-Sutcliffe efficiency value. Figure 9 shows the discrepancy plot of the log-polynomial (NS = 0.611) and power law equations (NS = 0.689) in comparison

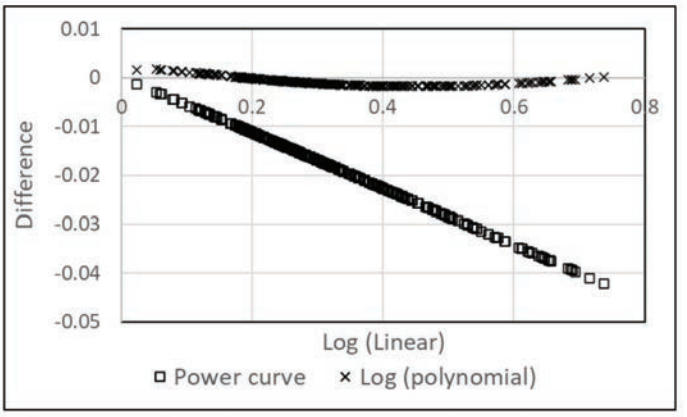

Figure 9: Discrepancy plot for FS4 (prediction for 2008) comparing the power law, log-transformed linear and log-transformed polynomial equations

with the log-transformed linear equation (NS = 0.607). The results of the both log-transformed equations are closely identical, whereas the power law shows larger differences.

Conclusion

This study examines the correlation between suspended sediment discharge and concentration to the streamflow in Langat River. It is found that the log-transformed linear equation fits the data well, where sediment peak discharge lag by one day. The phenomenon may be attributed to dispersed sediment sources and travel time. FS1 is located sufficiently upstream to have minimal sediment observation, while the catchments of FS2 and FS4 have approximately equal sediment contribution, hence higher total sediment loads are recorded in the downriver direction. However, streamflow dilution causes reduction in sediment concentration in FS4. The monthly sediment load variation is found to coincide with monsoon seasons and flash flood events. The latter can be identified as outliers in the plot of suspended sediment concentration in the flow duration curve. The seasonal and annual sediment load in the Langat River basin is estimated, where the annual total at FS4 is approximately 0.66 million tonnes. The SD prediction for years 2007 and 2008 show significant error during high flow events and thus the sediment load may be overly estimated.

Acknowledgements

The authors wish to acknowledge the financial support of FRGS Grant No. 600-IRMI/FRGS 5/3 (180/2019) by RMC of Universiti Teknologi MARA (UiTM), Malaysia. We would also like to thank the Department of Irrigation and Drainage Malaysia for providing the data that made this study possible.

References

Allen, P. A. (2008). From landscapes into geological history. *Nature*, *451*, 274-276. doi: 10.1038/nature06586.

Aminuddin Ab. Ghani, H. Md. Azamathulla, Chun Kiat Chang, Nor Azazi Zakaria & Zorkeflee Abu Hasan. (2011). Prediction of total bed material load for rivers in Malaysia: A case study of Langat, Muda and Kurau Rivers. *Environ Fluid Mech*, *11*, 307-318.

Atkinson, E. (1995). Methods for assessing sediment delivery in river systems. *Hydrological Scinces-Journal-des Sciences Hydrologiques*, *40*(2), 273-280. doi: 10.1080/02626669509491409.

Balamurugan, G. (1989). The use of suspended sediment rating curves in Malaysia: Some preliminary considerations. *Pertanika*, *12*(3), 367-376.

De Girolamo, A. M., Pappagallo, G., & Lo Porto, A. (2015). Temporal variability of suspended sediment transport and rating curves in a Mediterranean river basin: The Celone (SE Italy). *Catena*, *128*, 135-143. doi: 10.1016/j.catena.2014.09.020.

Hadi Memariana, Siva Kumar Balasundramb & Mohamad Tajbakhsh. (2013). An expert integrative approach for sediment load simulation in a tropical watershed. *Journal of Integrative Environmental Sciences*, *10*(3-4), 161-178.

Hassan, S. I. K. A. A. (2014). Suspended sediment rating curve for Tigris River upstream Al-Amarah barrage. *Int. Journal of Advanced Research*, *2*(5), 624-629.

He, X., & Jiao, J. (1998). The 1998 flood and soil erosion in Yangtze River. *Water Policy*, *1*, 653-658. doi: 10.1016/S1366-7017(99)00014-8.

Heng, S., & Suetsugi, T. (2015). Regionalization of sediment rating curve for sedimentyield prediction in ungauged catchments. *Hydrology Research*, *46*(1), 26-38. doi: 10.2166/nh.2013.090.

Horowitz, A. J. (2003). An evaluation of rating curves for estimating suspended sediment concentrations for subsequent flux

calculations. *Hydrol. Processes*, *17*, 3387-3409. doi: 10.1002/hyp.1299.

Letcher, R. A., Jakeman, A. J., Merritt, W. S., McKee, L. J., Eyre, B. D., & Baginska, B. (1999). *Review of techniques to estimate catchment exports*. Report EPA 99/73, Environment Protection Authority, Sydney, Australia.

Merritt, W. S., Latcher, R. A., & Jakeman, A. J. (2003). A review of erosion and sediment transport models. *Environmental Modelling and Software*, *18*, 761-799. doi: 10.1016/S1364-8152(03)00078-1.

Millman, J. D., & Meade, R. H. (1983). World-wide delivery of river sediment to the oceans. *The Journal of Geology, 91*(1), 1-21. The Uni. of Chicago Press.

Mishra, D., & Soni, D. (2019). Outlier detection for improving data robust by ODAD clustering technique. *International Journal of Advanced Trends in Computer Science and Engineering*, *8*(6), 3511-3519. doi: 10.30534/ijatcse/2019/130862019.

Moatar, F., & Meybeck, M. (2005). Compared performances of different algoritms for estimating annual nutrient loads discharged by the eutropic River Loire. *Hydrol. Processes*, *19*, 429-444. doi: 10.1002/hyp.5541.

Munodawafa, A. (2007). Assessing nutrient losses with soil erosion under different tillage systems and their implications on water quality. *Physics and Chemistry of the Earth*, *3*, 1135-1140. doi: 10.1016/j.pce.2007.07.033.

Mount, N. J., & Abrahart, R. J. (2011). Load or concentration, logged or unlogged? Addressing ten years of uncertainty in neural network suspended sediment prediction. *Hydrol. Processes*, *25*, 3144-3157. doi: 10.1002/hyp.8033.

Nyssen, J., Poesen, J., Moeyersons, J., Deckers, J., Haile, M., & Lang, A. (2003). Human impact on the environment in the Ethiopian and Eritrean highlands—A state of the art. *Earth-Science Review*, *64*, 273-320. doi: 10.1016/S0012-8252(03)00078-3.

Phillips, J. M., Webb, B. W., Walling, D. E., & Leeks, G. J. L. (1999). Estimating the suspended sediment loads of rivers in the LOIS study area using infrequent samples. *Hydrol. Processes*, *13*, 1035-1050. doi: 10.1002/(SICI)1099-1085(199905)13:7<1035::AID-HYP788>3.0.CO;2-K.

Rahman, M. R., Shi, Z. H., & Chongfa, C. (2009). Soil erosion hazard evaluation-An integrated use of remote sensing, GIS and statistical approaches with biophysical parameters towards management strategies. *Ecological Modelling*, *220*, 1724-1734. doi: 10.1016/j.ecolmodel.2009.04.004.

Rickson, R. J. (2013). Can control of soil erosion mitigate water pollution by sediments? *Science of the Total Environment*, *468-469*, 1187-1197. doi: 10.1016/j.scitotenv.2013.05.057.

Tfwala, S. S., & Yu, M. W. (2016). Estimating sediment discharge using sediment rating curves and artificial neural networks in the Shiwen River, Taiwan. *Water*, *8*(53), 1-15. doi: 10.3390/w8020053.

Wang, Y., & Ren, M. E. (1998). Sediment transport and terrigenos fluxes. In K. H., Brink & A. R., Robinson (Eds.), *The sea: Volume 10 - The global coastal ocean: Processes and methods*. (1st ed., pp. 253-292). New York, NY: John Wiley & Sons.

Xiao, X., White, E. P., Hooten, M. B., & Durham, S. L. (2011). On the use of log-transformation vs. nonlinear regression for analyzing biological power laws. *Ecology*, *92*(10), 1887-1894. doi: 10.1890/11-0538.1.

Yang, Chih Ted. (2003). *Sediment transport: Theory and practice*. Krieger Pub Co.

Yang, C. C., & Lee, K. T. (2018). Analysis of flow-sediment rating curve hysteresis based on flow and sediment travel time estimations. *Int.l Journal of Sediment*

Research, *33*, 171-182. doi: 10.1016/j.ijsrc.2017.10.003.

Zainal Abidin, M., Kutty, A. A., Lihan, T., & Zakaria, N. A. (2018). Hydrological change effects on Sungai Langat water quality. *Sains Malaysiana, 47*(7), 1401-1411. doi: 10.17576/jsm-2018-4707-07.

Zainal Abidin, R., Sulaiman, M. S., & Yusoff, N. (2017). Erosion risk assessment: A case study of the Langat River bank in Malaysia. *Int. Soil and Water Conservation Research*, *5*(1), 26-35. doi: 10.1016/j.iswcr.2017.01.002.